GATA4 regulates Fgf16 to promote heart repair after injury

Wei Yu[1], Xiuzhen Huang[1], Xueying Tian[1], Hui Zhang[1], Lingjuan He[1], Yue Wang[1], Yu Nie[2], Shengshou Hu[2], Zhiqiang Lin[3], Bin Zhou[4], William Pu[3], Kathy O. Lui[5], Bin Zhou[1,6,7*]

[1]Key Laboratory of Nutrition and Metabolism, Institute for Nutritional Sciences, Shanghai Institutes for Biological Sciences, Graduate School of the Chinese Academy of Sciences, Chinese Academy of Sciences, Shanghai, 200031, China.

[2]State Key Laboratory of Cardiovascular Disease, Fuwai Hospital, National Center for Cardiovascular Disease, Chinese Academy of Medical Sciences and Peking Union Medical College, Beijing 100037, China.

[3]Department of Cardiology, Boston Children's Hospital, 300 Longwood Ave, Boston, MA 02115, USA.

[4]Departments of Genetics, Pediatrics and Medicine (Cardiology), Albert Einstein College of Medicine of Yeshiva University, 1301 Morris Park Avenue, Bronx, NY 10461, USA.

[5]Department of Chemical Pathology, Li Ka Shing Institute of Health Sciences, The Chinese University of Hong Kong, Prince of Wales Hospital, Shatin, Hong Kong SAR, China.

[6]Institute of Neuroscience, State Key Laboratory of Neuroscience, CAS Center for Excellence in Brain Science and Intelligence Technology, Shanghai Institutes for Biological Sciences, Chinese Academy of Sciences, Shanghai, 200031, China.

[7]ShanghaiTech University, Shanghai, China

*Author for correspondence: zhoubin@sibs.ac.cn

SUMMARY

While the mammalian heart could regenerate during the neonatal stage, such an endogenous regenerative capacity is lost with age. Importantly, replication of cardiomyocytes is found to be the key mechanism responsible for neonatal cardiac regeneration. Unraveling the transcriptional regulatory network for inducing cardiomyocyte replication will, therefore, provide important insights into development of novel therapies to drive cardiac repair after injury. Here, we explored if the key cardiac transcription factor GATA4 is required for neonatal mouse heart regeneration. Using the neonatal mouse heart cryoinjury and apical resection models with an inducible loss of GATA4 specifically in cardiomyocytes, we found severely depressed ventricular function in the Gata4 ablated mice (mutant) after injury. This was accompanied with reduced cardiomyocyte replication. In addition, the mutant hearts displayed impaired coronary angiogenesis and increased hypertrophy and fibrosis after injury. Mechanistically, we found that the paracrine factor FGF16 was significantly reduced in the mutant hearts after injury compared with that of the littermate controls and was directly regulated by GATA4. Cardiac specific overexpression of FGF16 via adeno-associated virus subtype 9 (AAV9) in the mutant hearts partially rescued the cryoinjury-induced cardiac hypertrophy; promoted cardiomyocyte replication and improved heart function after injury. Altogether, our data demonstrated that GATA4 is required for neonatal heart regeneration through regulation of Fgf16, suggesting that paracrine factors could be of potential use in promoting myocardial repair.

KEY WORDS: Heart repair, Heart regeneration, Cardiomyocyte proliferation, GATA4, FGF16

INTRODUCTION

Myocardial infarction is becoming the leading cause of death worldwide. During myocardial infarction, a substantial number of cardiomyocytes die and cardiac hypertrophy occurs subsequently as a result of compensatory response. Lack of adequate numbers of functional cardiomyocytes coupled with chronic overload and subsequent dysfunction of the remaining cardiomyocytes eventually lead to heart failure and death. Since cardiomyocyte replication is the key mechanism by which the neonatal heart regenerates, unraveling the transcriptional regulatory network responsible for cardiomyocyte replication could provide important insights into development of novel therapies to drive cardiac repair after injury.

The GATA family members are zinc finger transcription factors. They bind specifically to the HGATAR-containing DNA motifs through their highly conserved zinc-finger DNA-binding domains (Patient and McGhee, 2002). Vertebrates have six GATA factors; and of which, GATA4 plays a key role during heart development. It regulates many cardiac specific genes that are critical for embryonic and neonatal heart growth (Monzen et al., 1999), including differentiation (Boheler et al., 2002), migration (Molkentin et al., 1997), hypertrophy (Charron et al., 2001; Liang et al., 2001) and survival (Aries et al., 2004) of cardiomyocytes. GATA4 also coordinates with a large number of cardio-regulators via the C-terminal zinc finger domain to maintain proper cardiac function throughout life (Durocher et al., 1997; Lu et al., 1999; Belaguli et al., 2000; Morin et al., 2000; Bhalla et al., 2001). Previous studies showed that GATA4 is critical in regulation of cardiac hypertrophy, cardiomyocyte viability and fibrosis during the adulthood (Bisping et al., 2006; Oka et al., 2006). In spite of the important function of Gata4 in heart development and homeostasis, the role of Gata4 involved in mammalian heart regeneration remains unknown.

Fibroblast growth factors (FGFs) are pluripotent growth factors; and are essential in cell proliferation and differentiation during organ development and tissue regeneration (Ornitz and Itoh, 2015). FGFs promote coronary angiogenesis during development and repair (Cross and Claesson-Welsh, 2001); and are also important for wound healing (Werner and Grose, 2003). FGFs play a pivotal role in development of multiple systems including the limb, lung and nervous system (Min et al., 1998; Ford-Perriss et al., 2001). Among all the family members, FGF16 belongs to the FGF9 subfamily; and is the only cardiac-specific member of the FGF family. FGF16 is mainly expressed in cardiomyocytes and could be secreted from cardiomyocytes after

birth, suggesting its specific role in the postnatal heart (Hotta et al., 2008). Previous study showed that FGF16 is required for cardiomyocyte replication during development (Lu et al., 2008). The expression level of FGF16 expression increases after birth and is stored in the extracellular matrix throughout the adulthood to maintain cardiac homeostasis and protect the heart from injury (Miyake et al., 1998; Hotta et al., 2008). Recent reports also showed that FGF16 protects the heart from doxorubicin-induced heart dysfunction (Sontag et al., 2013). Furthermore, Fgf16 is a direct target of NF-kB, which is involved in many cardiac pathological processes (Valen et al., 2001; Sofronescu et al., 2010). Altogether, previous findings indicate that FGF16 may play a direct role in protection of the neonatal heart.

In this study, we demonstrated that cardiomyocyte specific ablation of Gata4 resulted in compromised regenerative capacity in the neonatal heart with decreased proliferating cardiomyocytes following apical resection and cryoinjury. We also found that GATA4 regulated Fgf16 expression. Experimental over-expression of FGF16 via AAV9 in cardiomyocytes partially rescued the phenotype of Gata4 ablation, suggesting that the Gata4-Fgf16 axis could regulate neonatal heart regeneration.

MATERIALS AND METHODS

Animal procedures

All animals were used according to guidelines from the Institutional Animal Care and Use Committee of the Institute for Nutritional Sciences, Shanghai Institutes for Biological Sciences, Chinese Academy of Sciences. We crossed the iTnt-Cre mice, in which the troponin T promoter drives the reverse tet activator protein (rtTA) and the tet activator protein-dependent (TRE) promoter drives the Cre recombinase (iTNT-Cre) (Wu et al., 2010), with the Gata4$^{fl/fl}$ mice (Watt et al., 2004), in which the 3/4/5 exon of Gata4 is flanked by Loxp sites, to generate rtTA-Cre; Gata4$^{fl/fl}$ mice with specific deletion of the Gata4 3/4/5 exon after doxycycline (Dox) administration. All animals were performed in blind for treatments and analyses. Pregnant mice at E16.5 were injected intragastrically once daily for 3 days with doxycycline, Dox (10 mg/ml; 10 μl per gram of body weight) (Sigma, D9891-25G) to activate the Cre.

Neonatal mouse heart cryoinjury (CI)

Neonatal mice at postnatal day 1 (P1) were subjected to frozen anesthesia for about 3-5 minutes, and then were placed on the frozen operation table after breathing steady. 70% alcohol was used to disinfect the surgical site and the mouse limbs were fixed with forceps. Approximately 1 cm incision was generated along the sternum and vertical of the chest muscles under the stereo-microscope. 2-3 intercostal incisions were made in the left sternum chest to separate the pericardium and expose the left ventricle of the heart. 1mm blunt port copper wire was prepared and frozen to -70 ℃; and was then put on the left ventricle of frostbite and maintained for approximately 7-8 seconds until the left ventricle appeared as white in color. After injury, the bubbles and blood in chest were squeezed out and chest was sewn up with 8-0 sutures and the skin was closed with 11-0 sutures. After the operation, the neonatal were placed under 37 ℃ lamp to keep warm. They were then placed back to the feeding mice as soon as possible as soon as they woke up with the color of the skin returned to normal. In the sham-operated group, we performed the same experimental procedures as above except that we replaced liquid nitrogen with PBS at room temperature.

Neonatal mouse heart apical resection (AR)

The neonatal mouse heart AR injury model was performed as described previously (Porrello et al., 2011; Han et al., 2015). Briefly, neonatal mice at postnatal day 1 (P1) were subjected to frozen anesthesia for 3 – 5 minutes, and the mice were placed on the frozen operation table after breathing steady. 70% alcohol was used to disinfect the surgical site and the mouse limbs were fixed with forceps. Approximately 1 cm incision was generated and the sternum vertical of the chest muscles was separated under the stereo microscope. 2 – 3 intercostal incisions were made in the left sternum chest to separate the pericardium and expose the apex. Curved forceps were extended into the intrathoracic to pull heart out and the apex was truncated with microsurgical scissors. The bubbles and blood in chest were squeezed out and the chest was sewn up with 8-0 sutures, and the skin was sewn up with 11-0 sutures. After the operation, the neonatal mice were placed under 37 ℃ lamp to keep warm. Then mice were placed back to the feeding mice as soon as they woke up with the skin retured to normal color. In the sham-operated control, we performed the same experimental procedures as above except that we did not truncate the heart apex.

Echocardiography

The left ventricle systolic function was measured two months following cryoinjury with echocardiography in mice via a digital ultrasound system (Vevo2100 Imaging System, VisualSonics). Conventional measurements of the left ventricle (LV) included: end-diastolic diameter (LVEDD), end-systolic diameter (LVESD), intraventricular septal thickness (IVST) and posterior wall thickness (LVPWT), ejection fraction (LVEF), as well as fractional shortening (LVFS).

Western blot

Heart tissues were collected and dissected at the indicated stages. Tissues were homogenized in Tris-SDS lysis buffer (50 mM Tris pH8.0 and 1% SDS) and incubated at room temperature for 20 minutes, followed by centrifugation at maximum speed to get the protein supernatant. All protein samples were mixed 1:4 with 4xLoading buffer (10% SDS, 1.5 M dithiothreitol and 0.3 M Tris-HCl pH6.8) and boiled for 5 minutes. Proteins were resolved by 10% SDS PAGE and transferred onto a polyvinylidene fluoride (PVDF) membrane (Immobilon, Millipore, Billerica,

MA) using a Mini Trans Blot system (Bio-Rad). The membranes were then blocked in TBS-T (10 mM Tris-HCl pH8.0, 150 mM NaCl and 0.5% vol/vol Tween-20) containing 5% skim milk powder at room temperature for 1 hour. After that, membranes were incubated with the indicated primary antibody at 4 °C overnight. In the next day, membranes were washed and then incubated with HRP conjugated secondary antibody at room temperature for 1 hour. Signals were detected by enhanced chemiluminescence (Pierce) according to manufacturer's instructions. Antibodies used for Western Blot in this study included: anti-GATA4 (Santa Cruz, sc-1237), anti-FGF16 (Santa Cruz, sc-376214), anti-beta-actin (Cell Signaling, 4970L), HRP-anti-rabbit IgG (JIR, 711-035-152), HRP-anti-mouse IgG (JIR, 115-035-174), and HRP-anti-goat IgG (JIR, 705-035-147).

Quantitative RT-PCR (qRT-PCR) analysis

Heart tissues were collected and dissected at the indicated stages. RNA was extracted with Trizol according to manufacturer's instructions (Invitrogen); and then converted to cDNA using the PrimeScript™ RT reagent Kit with gDNA Eraser (Takara, RR047A). For qPCR, the SYBR Green qPCR master mix (Applied Biosystems) was used and cDNA was amplified on 7500 Real-Time PCR System (Applied Biosystems). A list of PCR primers is included in supplementary material Table S2.

Histology

Murine hearts were collected at the indicated stages and fixed in 4% paraformaldehyde at 4 °C for 30 minutes. The heart tissues were dehydrated in 30% sucrose at 4 °C overnight and embedded with OCT at -80 °C for 30 minutes. Frozen sections were prepared in 10 μm and collected on slides. Sirius Red/Fast Green staining was performed to determine collagen deposition: cryosections/slides were washed in PBS and fixed in 4% paraformaldehyde for 10 minutes. Slides were then incubated in Bouins' solution (5% acetic acid, 9% formaldehyde and 0.9% picric acid) at room temperature overnight. Next day after washing, slides were incubated in 0.1% Fast Green (Fisher, F-99) for 3 minutes, then in 0.1% Sirus Red (Direct red 80, Sigma, 0-03035) for 2 minutes. After wash for 3 times, slides were dehydrated with ethanol and xylene based on standard procedures. Hematoxylin/Eosin staining was also performed according to standard procedures as previously described (He et al., 2014). Images were taken and quantified based on this formula: Scar perimeter/Total

perimeter. Images were acquired on either a Leica M165 FC stereo microscope or an Olympus BX53 microscope.Images were analyzed and quantified based on this formula: Scar perimeter/Total perimeter.

EdU pulse-chase

For EdU (5-ethynyl-2'-deoxyuridine) labeling experiments, the EdU solution dissolved in sterile 0.9% saline, at the dose of 10 µg/g, was injected subcutaneously in neonates on days 1 and 7 after surgery. Hearts were collected and sectioned at 7 days after surgery. EdU staining was then performed based on LifeTech CLICK EDU ALEXA 488 IMAGING kit protocol (Life, C10337).

Immunostaining

Cryosections/slides were washed in PBS and fixed in 4% paraformaldehyde for 10 minutes. Slides were blocked in PBS containing 0.1% Triton X-100 and 5% normal donkey serum (PBSST) at room temperature for 1 hour. Followed by first antibody incubation at 4 °C overnight, signals were developed with Alexa Fluor secondary antibodies at room temperature for 30 minutes. Before mounting, tissues were counterstained with DAPI. Slides were examined by fluorescence microscopy (Olympus DP72) or laser confocal (510 META, Carl Zeiss) microscopy, as indicated where appropriate. Antibodies used in immunofluorescence for this study included: anti-GATA4 (Santa Cruz, sc-1237), anti-a-Actinin (Sigma, A7811), anti-Phospho-histone H3 (Upstate, 06-570), Ki67 (lab vision, RM-9106-F1), EdU(life, C10337), WGA-Alex555 (invitrogen, W32464), anti-smooth muscle actin-fitc (Sigma, F3777), anti-PECAM (BD, 553370), donkey anti-mouse 555 (invitrogen, A31570), Alexa donkey anti-goat 488 (invitrogen, A11055), Alexa donkey anti-rabbit 555 (invitrogen, A31572), and donkey anti- rat 594 (invitrogen, A21209). For weak signals, we used HRP or biotin-conjugated secondary antibodies and a tyramide signal amplification kit (PerkinElmer). Images were acquired on Olympus BX53 microscope. Quantification of all experiments was performed by an observer blinded to the experimental design.

ChIP-qPCR

ChIP-qPCR assays were performed using the chromatin immunoprecipitation assay kit (Millipore, #17-295) per manufacturer's instructions. Briefly, a 15 cm plate of

C2C12 cells which expressed GATA4 or mouse heart pieces were treated with 1% formaldehyde at room temperature for 15 minutes to crosslink protein and DNA complex. After washed with PBS 3 times, tissues were homogenized and cells were then lysed and sonicated to shear the DNA into 200-600 bp fragments. The supernatant was incubated with 4 μg of anti-GATA4 antibody (Santa Cruz, sc1237) or 4 μg anti-goat immunoglobulin G (IgG) (Santa Cruz, sc2020) overnight at 4 °C. The DNA fragments were then precipitated with beads for 1 hour and were recovered following the manufacturer's protocol. Primers used in ChIP-qPCR were listed in supplementary material Table S2. For Cdk4, regions of GATA4 sites were amplified as previously described (Rojas et al., 2008).

Primary cell culture

Neonatal mouse cardiomyocytes were collected and isolated using the Neonatal Rat/Mouse Cardiomyocyte Isolation Kit (Cellutron, nc-6031) per manufacturer's instructions. Briefly, postnatal day 1 (P1) ventricles of C57Bl/6 mice were minced and dissociated by several trypsinization steps at 37 °C. Non-cardiomyocytes were separated from cardiomyocytes by the method of differential plating. Cardiomyocytes were then cultured in 24-well plate for 24 hours before transfection.

Luciferase activity measurement

Fragments were amplified by each primer pairs listed in supplementary material Table S2. Each fragment was cloned into the pGL3-basic reporter vector. Neonatal mouse cardiomyocytes (NMVMs) were cultured in 24-well plates and were transfected with 500 ng/well of the indicated plasmid and 50 ng/well pRC-RSV-ßGal (internal control vector) via 2 μl lipofectamine 3000 (Invitrogen) for the luciferase activity assay. Luciferase activity was measured 36 hours after transfection using the Dual-Luciferase reporter assay system (Promega, E1910) per manufacturer's instructions. ß-Gal activity was detected by the SpectraMaxPlus plate reader at A420 nm based on Ernie's beta-Gal assay protocol.

AAV9 packaging and delivery

Luciferase, GFP-Cre and mouse Fgf16 were seperately cloned into the ITR-containing AAV9 plasmid (Penn Vector Core P1967) respectively, which was driven by the cardiac TNT promoter, to yield pAAV.cTnT::Luciferase, pAAV.cTnT::GFP-

Cre, pAAV.cTnT::Fgf16, respectively. AAV9 were packaged in 293T cells with AAV9:Rep/Cap and pAd:deltaF6 (pHelper) as described previously (Grieger et al., 2006; Lin et al., 2014). AAV9 were then purified and concentrated by gradient centrifugation. Titer was determined by quantitative PCR. AAV9 were dissolved in PBS and injected subcutaneously into neonatal mice after cryoinjury and 6 days post injury.

Statistics

Data for two groups were analyzed by an unpaired student's *t* test, while comparison between more than two groups was performed using an ANOCA followed by Tukey's Multiple Comparison Test. Significance was accepted when $P < 0.05$. All data are presented as mean ± s.e.m.

RESULTS

Inducible cardiomyocyte-specific deletion of Gata4

To study the role of Gata4 in neonatal heart regeneration, we generated a model of inducible deletion of Gata4 in cardiomyocytes at the perinatal stage. We used the iTNT-Cre mouse, in which the cardiac-specific troponin T promoter drives the reverse tet activator protein (rtTA) and the tet activator protein-dependent (TRE) promoter drives the Cre recombinase (Fig. 1A). Administration of doxycycline (Dox) upregulates Cre expression in cardiomyocytes, resulting in Cre-mediated recombination of the floxed targets (Wu et al., 2010). We next generated the iTnt-Cre; $Gata4^{fl/fl}$ mice (mutant), which specifically delete Gata4 3/4/5 exon in cardiomyocytes (Watt et al., 2004) after intragastrical administration of Dox during the perinatal stages (embryo day 16.5 to 18.5, Fig. 1A). For the control, we crossed the non transgene (Ntg) bearing iTNT-Cre negative littermates with the $Gata4^{fl/fl}$ mice, which received the same Dox treatment. We next introduced cryoinjury in neonatal mice as the cryoinjury model provides a scar of consistent size and shape to obviate the injury variance between animals. (Strungs et al., 2013). By masson trichrome staining and sirius-red staining to localize fibrotic tissues, we found scar formation in the neonatal heart 5 days after cryoinjury (Fig. 1B). We also confirmed formation of fibrotic tissues in the cryoinjury region by immunostaining of the fibrosis marker collagen III (COL3) and cardiomyocyte specific marker ACTN2 (Fig. 1B), demonstrating the successful establishment of cryoinjury in neonatal hearts. In order to test the efficiency of ablating Gata4 in neonatal hearts, we collected mutant and control hearts at postnatal day 4, and analyzed Gata4 expression by quantitative reverse transcription PCR (qRT-PCR). We found that the *Gata4* mRNA was significantly reduced in the Gata4 mutant group compared with that of the littermate controls (Fig. 1C). To further validate deletion of GATA4 at the protein level, we performed western blot using lysates from mutant and control hearts and confirmed that GATA4 was significantly reduced in the mutant group compared with that of the controls (Fig. 1D). To provide the knockout information on single cell resolution, we performed co-staining of GATA4 and ACTN2 on the mutant and control hearts. Compared with the control hearts, GATA4 was not expressed in the majority of cardiomyocytes in the mutant hearts (Fig. 1E). Quantification of the number of GATA4-expressing cardiomyocytes showed that GATA4 was deleted in over 90% cardiomyocytes of the mutant hearts (Fig. 1F). Altogether, we established the neonatal cardiomyocyte-

specific Gata4 ablation model and cryoinjury model, allowing us to test if GATA4 is required for recovery and heart regeneration after injury.

GATA4 is required for neonatal heart repair after cryoinjury

We next evaluated the regenerative capacity of the Gata4-ablated neonatal hearts by examining their function at the adult stage. After Dox treatment from embryo day (E) 16.5 to E18.5, we performed cryoinjury on neonatal murine hearts at postnatal day 1 (P1) and measured heart function by echocardiography 8 weeks after cryoinjury. Gross morphology showed that there was an obvious scar formation in the mutant heart, which was less visible in the controls (Fig. 2A). We also found compromised heart function and significantly decreased fractional shortening in the mutant mice compared to that of the littermate controls by echocardiographic measurements (Fig. 2B, C and supplementary material Table S1). Interestingly, we found that heart function was normal in the sham-operated Gata4 knockout hearts at 8 weeks, indicating that cardiomyocytes could function normally without GATA4 in the absence of injury (Fig. 2C and supplementary material Table S1). By sirius red and fast green staining on heart sections, we found that the area of scar tissues was significantly larger in the mutant hearts compared to that of the controls (Fig. 2D). Quantitative of scar size measured as a percentage of ventricular circumference in sequentially stained sections showed a significantly larger scar formed in the mutant hearts compared to that of the controls (Fig. 2E). To examine if deletion of GATA4 in cardiomyocytes results in cardiomyocyte hypertrophy of the adult hearts after injury, we co-stained lectin-specific marker WGA and muscle-specific actinin marker ACTN2 on mutant or control heart sections to visualize the size of individual cardiomyocyte. We found that the mean size of cardiomyocytes of mutant hearts was larger than that of the controls (Fig. 2F,G). Together, our data suggested that GATA4 might be required in heart regeneration and functional maintenance after cryoinjury.

GATA4 is required for neonatal heart repair after apical resection

We further applied a second injury model, apical resection (AR), to test weather Gata4 is required during heart regeneration. We first treated mice with Dox at perinatal period and removed the heart apex from neonatal mouse heart as previously described (Porrello et al., 2011). Echocardiographic measurements of mouse hearts showed that the heart function of mutant mice did not recover completely compared

to that of the littermate controls after AR (Fig. 3A,B). Sirius Red staining on sagittal heart sections showed that there were still fibrotic scar tissues in the apical area of the Gata4 mutant hearts, which failed regenerate the apex completely; while the littermate control hearts completely recovered after injury (Fig. 3C), which is consistent with the original report (Porrello et al., 2011). We next ask whether reduced cardiac regeneration post AR was due to impaired cardiomyocyte replication in the cardiomyocyte-specific Gata4-ablated mice. To address this issue, we utilized proliferation markers pH3, Ki67 and EdU incorporation to study cardiomyocytes proliferation 7 days after AR. Quantification of proliferating cardiomyocytes showed that replicating cardiomyocytes were significantly reduced in both the border zone and remote region of the mutant hearts compare to that of the littermate controls (Fig. 3D-H). However, there is no significant difference in the proportion of proliferating cardiomyocyte number in sham-operated mutant hearts and littermate control hearts (Fig. 3D-H).

GATA4 is required for cardiomyocyte replication and repair post cryoinjury

To examine if Gata4 induced heart regeneration by promoting cardiomyocyte replication in cryoinjury model, we measured cardiomyocyte replication at P7 with the phosphor-histone H3 (pH3) antibody on heart sections as previously described (Porrello et al., 2011). We found that the pH3 positive proliferating cardiomyocytes were dramatically reduced in both the border zone and remote region of the mutant hearts compared to that of the controls (Fig. 4A-C). We next used AurkB antibody to detect cardiomyocyte cytokinesis during proliferation. We found that the number of cardiomyocytes undergoing cytokinesis was significantly reduced in mutant hearts compared to that of the controls (Fig. 4D,E). Since previous work suggested that cardiomyocytes of the whole heart replicate to compensate for the loss of cardiomyocytes in the neonatal stage after injury (Porrello et al., 2011), our results might indicate that a loss of GATA4 in cardiomyocytes could lead to reduced regenerative response of the whole heart (both border zone and remote region) after injury.

We then measured the expression levels of genes regulating cell cycle progression, such as *Cyclin A2*, *Cdk4*, *Cyclin D1* and *Cyclin D2*, of both the mutant and control hearts. While *Cyclin D1* and *Cyclin D2* were not significantly changed in the mutant hearts, the expression levels of *Cyclin A2* and *Cdk4* were reduced in the mutant heart

compared to that of the controls (Fig. 4F). Indeed, it has been reported that CDK4 is essential for cardiomyocyte replication; and is directly regulated by GATA4 (Rojas et al., 2008). To confirm if GATA4 directly binds to the *Cdk4* promoter, we cloned the *Cdk4* promoter into a luciferase reporter plasmid. Co-transfection of the Gata4-expressing plasmids promoted *Cdk4* promoter-driven luciferase expression (Fig. 4G). We next performed chromatin immunoprecipitate (ChIP) assays on C2C12 cell line and confirmed that GATA4 bound to the *Cdk4* promoter (Fig. 4H). To test whether the GATA4 binding was enhanced after injury, we used sham-operated and cryo-injured heart lysates for ChIP assays. Gata4 knockout hearts from sham-operated mice were used as negative control. We found that GATA4 mainly bound to site III in the normal heart lysates. Notably, the binding of the site I/II but not site III was significantly increased after cryoinjury (Fig. 4I). Taken together, our results suggested that GATA4 might be required for increased cardiomyocyte replication during neonatal heart regeneration in response to injury, possibly by regulating expression of the cell cycle protein CDK4.

GATA4 is required for coronary angiogenesis during neonatal heart regeneration

Previous report indicates that GATA4 functions as a stress-responsive regulator of coronary angiogenesis (Heineke et al., 2007). To test if cardiomyocyte GATA4 functions in regulation of coronary angiogenesis during heart regeneration, we compared the coronary vessel numbers in mutant hearts with the controls after cryoinjury. By immunostaining of endothelial cell specific marker PECAM, we found a significant reduction in the capillary to cardiomyocyte ratio in the mutant hearts compared to that of the controls (Fig. 5A,B), suggesting that each cardiomyocyte in mutant hearts was supported by fewer coronary capillaries in the mutant hearts. We did not observe a significant reduction of capillary vessels in the mutants compared to that of the sham-operated controls (Fig. 5B). Moreover, we also performed immunostaining of the smooth muscle cell specific marker alpha SMA on heart sections of the mutant and control hearts; and found a significant reduction in the number of small coronary arteries in the mutant hearts compared to that of the controls, suggesting that loss of GATA4 in cardiomyocytes might also impair arteriogenesis and maintenance of vasculature after injury (Fig. 5C,D). There was no significant reduction of $aSMA^{+}$ coronary vessels in sham-operated mutant hearts

compared to that of the sham-operated control hearts (Fig. 5D). To further identify the pro- or anti-angiogenic genes associated with this phenotypic change, we measured the mRNA expression levels of ventricles of the mutant and control hearts. By qRT-PCR, we found that expression levels of a subset of pro-angiogenic genes such as members of the *Fgf* family (*Fgf2*, *Fgf9*, *Fgf16*) were significantly down-regulated; whereas expression levels of members of the *Vegf* family (*Vegfa*, *Vegfb* and *Vegfc*) were not significantly changed after ablation of GATA4 (Fig. 5E). Moreover, we also observed that the expression levels of some anti-angiogenic genes or fibrosis-associated genes, such as tissue inhibitor of metalloproteinase 1 (*Timp1*), collagen type IV, alpha 3 (*Col4a3*), connective tissue growth factor (*Ctgf*) and thrombospondin 1 (*Thbs1*) were significantly up-regulated in the mutant group compared to that of the controls (Fig. 5E). Among these genes, the pro-antiogenic *Fgf16* and anti-angiogenic *Ctgf* were down-regulated and up-regulated, respectively, in sham-operated mutant hearts compared to that of the littermate controls (Fig. 5E). Our data suggested that Gata4 could possibly regulate coronary angiogenesis during neonatal heart regeneration.

GATA4 directly regulates Fgf16 and FGF16 supplement partially rescues the mutant phenotype

Since several FGF family members were down regulated in cardiomyocytes with Gata4 ablation, we next examined expression levels of other FGF members in both mutant and control hearts and found that *Fgf2*, *Fgf3*, *Fgf8*, *Fgf9*, *Fgf16* were significantly down-regulated in the mutant hearts compared to that of the controls (Fig. 6A). Among these altered paracrine factors, it has been reported that FGF16 is essential for cardiomyocyte replication in the embryonic heart (Hotta et al., 2008). Therefore, we examined the protein expression level of FGF16 in the mutant and control hearts using western blots, we found that there was a significant reduction in the expression level of FGF16 protein in the mutant hearts compared to the controls after injury (Fig. 6B). Using the ECR browser (http://ecrbrowser.dcode.org), we found the conserved sequence of Fgf16 among the mouse, opossum and human genomes; and an evolutionarily conserved GATA binding motif on the second intron of Fgf16 gene (Fig. 6C). Next we cloned the Fgf16 promoter as well as its second intron into the luciferase reporter constructs; and co-transfect the Fgf16-luciferase reporter with Gata4 or p300 into neonatal mouse cardiomyocytes (NMVMs) (Fig. 6D).

Our data showed that GATA4 simulated the enhancer activity of Fgf16. When cotransfected with Gata4 and P300, as P300 is known as a GATA4 activator (Yanazume et al., 2003), expression level of the reporter was significantly enhanced with a nearly 5-fold increase compared to that of the control which was transfect with GFP-expressing construct (Fig. 6D). To validate this, we further used neonatal mouse hearts to perform chromatin immunoprecipitation followed by quantitative PCR (ChIP-qPCR), primers including the GATA4 binding sites and the control nonspecific sites were used (supplementary material Table S2). Our results confirmed that the GATA4 binding site was specifically found in the conserved region of the Fgf16 second intron (Fig. 6E). To measure the transcriptional activity of the GATA4-bound region of Fgf16, we cloned a 460 bp genomic DNA fragment containing the conserved GATA4 binding motif into a luciferase reporter construct, here we refer to as Fgf16 enhancer (EN); and a control mutant version (mEN) with a potentially muated Gata4 binding site (Fig. 6F). When Gata4 was transfected into NMVMs, we found that GATA4 stimulated the transcriptional activity of the Fgf16 enhancer nearly 3 fold. However, this stimulation could not be detected in the mutant enhancer control (Fig. 6F). Together, our results suggested that GATA4 directly bound to the evolutionary conserved site located on the second intron of the Fgf16 gene for regulating Fgf16 expression in neonatal cardiomyocytes.

Since previous study showed that FGF16 is critical for cardiomyocyte proliferation during development (Hotta et al., 2008), we asked if supplementing FGF16 into the mutant heart could rescue the phenotype caused by the loss of GATA4 in neonatal cardiomyocytes. Therefore, we generated the adeno-associated virus 9 :cTNT::Fgf16 virus (AAV9:Fgf16), in which expression of the Fgf16 was driven by the cardiomyocyte specific cTNT promoter and the plasmid was packaged into AAV9, a virus that targets cardiomyocytes efficiently and specifically (Lin et al., 2014). We first used AAV9:cTNT::GFP-Cre (AAV9:GFP-Cre) to evaluate the transduction efficiency and specificity in the Rosa26$^{RFP/+}$ reporter mouse. As expected, strong RFP signal was found specifically in the heart but not in other organs of the Rosa26$^{RFP/+}$ reporter mice following infection with the AAV9:GFP-Cre at neonatal stage (Fig. 6G). Immunostaining of the genetic lineage-tracing marker RFP and ACTN2 on the transduced Rosa26$^{RFP/+}$ heart sections showed that RFP was specifically expressed in the ACTN2 positive cardiomyocytes and the transduction efficiency was high as the majority of cardiomyocytes were labeled by RFP (Fig. 6G). After establishing the

efficient AAV9 transduction system, we injected the AAV9:Fgf16 virus subcutaneously into wild type neonatal mice at postnatal day 1 (P1) and injected again at P6, we then collected the hearts for analysis at P9 and examined the expression of FGF16. Here we used AAV9:cTNT::Luciferase (AAV9:Luci) as negative control. Our results from western blot of FGF16 showed that the FGF16 protein in AAV9:Fgf16 transduced hearts was 1.5 folds higher than that of the AAV9:Luci transduced controls (Fig. 6H). We next adopted the same delivery strategy for the mutant mice and tested if overexpression of FGF16 in cardiomyocytes could have any effect on expression of hypertrophy-associated genes after Gata4 knockout and injury in neonatal heart. Using qRT-PCR, we found that there was a significant reduction in expression of hypertrophy-associated markers including *Nppa*, *Nppb, Acta and Fhl1* in the mutant hearts transduced with the AAV9:Fgf16 virus compared to that transduced with the AAV9:Luci virus (Fig. 6I,J). Gene expression levels of the cell cycle markers such as *Ki67*, *Cdk4* and *Cyclin A2* were also upregulated in the AAV9:Fgf16 transduced mutant hearts compared to that of the AAV9:Luci transduced group (Fig. 6K). In addition, expression level of the apoptosis marker *Gdl15* was also significantly down regulated in the AAV9:Fgf16 transduced mutant hearts compared to that of the AAV9:Luci transduced group (Fig. 6K), suggesting that FGF16 possibly protected cardiomyocytes from cryoinjury-induced cell death. Furthermore, immunostaining of the proliferation markers pH3 and Ki67 on heart sections also showed that overexpression of FGF16 in the Gata4 ablated cardiomyocytes significantly promoted cardiomyocyte replication after injury (Fig. 6L-O). Our results revealed that supplement FGF16 to the Gata4 knockout hearts could significantly inhibit hypertrophy and promote proliferation of cardiomyocytes after injury.

FGF16 supplement rescues function of the Gata4 ablated heart

To determine the long term effect of FGF16 supplement in rescuing heart function followed by cardiomyocyte-specific Gata4 ablation, we repeated the same AAV9 delivery experiment as above, and analyzed heart function of the AAV9:Fgf16- or AAV9:Luci-transduced iTNT-Cre; $Gata4^{fl/fl}$ hearts until 8 weeks old. Our results of echocardiography showed that FGF16 supplement partially rescued the function of mutant hearts, as the ejection fraction and fraction shortening were significantly increased in the AAV9:Fgf16- compared to that of the AAV9:Luci-transduced hearts

of the iTNT-Cre; Gata4$^{fl/fl}$ mice (Fig. 7A,B). We also found that over-expression of FGF16 in sham-operated mutant or littermate control hearts did not impair heart function (Fig. 7B). We next measured the fibrotic scar size by staining of sirius red and fast green on heart sections. Compared with the AAV9:Luci transduced hearts, a significantly reduction in scar formation was observed in the AAV9:Fgf16 transduced hearts (Fig. 7C,D). Furthermore, we performed costaining for WGA and ACTN2 in the AAV:Fgf16 and AAV:Luci transduced hearts to measure cardiomyocyte size. We found that Fgf16 supplement reduced the size of cardiomyocytes in mutant hearts compared to that of the AAV:Luci controls (Fig. 7E,F). To investigate the effect of AAV9:Fgf16 on cardiomyocyte death, we performed costaining for terminal deoxynucleotidyl dUTP nick-end labeling (TUNEL) and ACTN2 to measure the number of apoptotic cardiomyocytes in the border region of the injured heart. We found that there were significantly fewer apoptotic cardiomyocytes in the AAV9:Fgf16 transduced hearts compared to that of the AAV9:Luci controls (Fig. 7G,H). Taken together, our study showed that FGF16 could partially rescue the impaired regenerative capability of the neonatal mouse heart following the cardiomyocyte specific ablation of Gata4, at least in part, by inhibiting hypertrophy and apoptosis of cardiomyocytes; reducing scar tissue formation; stimulating replication of cardiomyocytes; and improving heart function after injury.

DISCUSSION

There are several conserved transcriptional networks that orchestrate the delicate gene expression during heart development and growth. Previous work reported that GATA4 is essential for heart development (Wang et al., 2013) and postnatal maintenance (Bisping et al., 2006). Overexpression of GATA4 was reported to rescue injured heart after myocardial infarction (MI), by promoting myocardial angiogenesis; preventing heart remodeling; reducing apoptosis and ultimately leads to reduction of infarct size (Rysa et al., 2010). Here we used an inducible cardiomyocyte specific gene knockout strategy to generate cardiomyocyte specific and inducible Gata4 knockout mice. This strategy allowed us to ablate Gata4 in over 90% cardiomyocytes after birth and could also avoid early lethality and other embryonic phenotypes accompanied by early embryonic deletion of Gata4 (Zeisberg et al., 2005). Our data suggested that the heart functioned normally after Gata4 deletion in cardiomyocytes at the perinatal stage; however, the mutant heart regenerated poorly after cryoinjury compared to their littermate controls. We further showed that the impairment of heart regeneration was associated with a reduced amount of proliferating cardiomyocytes and coronary vessels, demonstrating a pivotal role of GATA4 during neonatal heart regeneration.

In addition to cryoinjury, we also utilized the apical resection (AR) strategy to induce neonatal heart injury. In line with the cryoinjury model, we found that Gata4 was essential for heart regeneration after AR. Although the neonatal mouse heart regenerated from injury in both models, the response and the degree of regeneration appeared to vary. We found that some fibrotic tissues remained after recovery from cryoinjury, while there was hardly any detectable scar tissue left in the AR model. Moreover, we also observed cardiomyocyte hypertrophy only in the cryoinjury model but not in AR, suggesting that the neonatal mouse heart could maintain function in response to the respective form of injuries via different mechanisms. For instance, the neonatal heart failed in eliminating excessive scar tissues post cryoinjury due to some secondary responses such as inflammation; and, therefore, different injury models might stimulate distinctive endogenous mechanisms for scar tissue regression after injury (Gonzalez-Rosa et al., 2011). Furthermore, the incomplete regeneration following cryoinjury in the neonatal heart could also be attributed to the severity of injury or size of damaged tissue during experiment procedures (Sen and Sadek, 2015), as demonstrated by previous study that complete regeneration is observed following

mild but not severe cryoinjury (Jesty et al., 2012). Nevertheless, our work suggested that the loss of Gata4 resulted in more severe cardiomyocyte hypertrophy with reduced cardiac function.

The molecular regulation of cardiac regeneration begins to be extensively studied recently. In zebrafish regeneration model, subepicardial ventricular cardiomyocytes trigger expression of Gata4 within a week of trauma (Kikuchi et al., 2010), and subsequent functional studies convincingly showed that the activation of Gata4 in the cortical myocardial layer is essential for shaping heart morphogenesis during heart regeneration (Gupta et al., 2013). In contrast to expression of Gata4 in the cortical myocardial layer of zebrafish heart (Gupta and Poss, 2012; Gupta et al., 2013), Gata4 is expressed throughout the ventricular myocardium of the neonatal mouse heart during homeostasis and after injury. In addition, the adult zebrafish heart retains the capability to regenerate, while the adult mammalian heart does not regenerate sufficiently to recover from significant injury such as myocardial infarction. Therefor, the neonatal mouse heart injury models induced by cryoinjury or apex resection represent interesting models for studying mammalian cardiac regeneration (Porrello et al., 2011; Sadek et al., 2014). Recent studies showed that a homeodomain transcription factor Meis1 is critical in regulation of neonatal myocyte proliferation and neonatal heart regeneration (Mahmoud et al., 2013). In addition to transcriptional regulation, microRNA (miR-15) also modulates neonatal heart regeneration through inhibition of postnatal cardiomyocyte proliferation (Porrello et al., 2013). These advances in the molecular regulation of neonatal mammalian heart regeneration, together with valuable information from adult zebrafish regeneration models, provide important insights into development of novel therapies to drive cardiac repair after injury.

In the cardiomyocyte-specific Gata4 ablated hearts, we also found that the number of capillaries and small vessels was reduced compared to that of the control hearts. Both the FGF and VEGF family members are crucial angiogenic factors that simulate survival, proliferation and differentiation of endothelial cells (Cross and Claesson-Welsh, 2001). Our qRT-PCR data revealed that the gene expression levels of the FGF family members, such as *Fgf2, Fgf3, Fgf8, Fgf9 and Fgf16* were significantly reduced, while the gene expression levels of the VEGF family (*Vegfa*, *Vegfb* and *Vegfc*) were not significantly changed after Gata4 knockout. These data suggested that GATA4 regulated vessel formation via the FGF pathway at least around the transient

regenerative window after birth. One caveat in interpretation of our data is that there is a change of expression pattern in pro- or anti-antiangiogenic genes in the sham-operated hearts compared to that of the littermate controls, eg. *Fgf16* and *Ctgf*. Our findings suggested that Gata4 regulates a subset of pro-angiogenic genes at the baseline, in addition to its important role as a stress-responsive regulator as revealed by the gain-of-function model (Heineke et al., 2007). However, we did not detect a significant reduction of capillaries or arteries in the mutant heart during homeostasis, nor did we observe any reduction of cardiomyocyte proliferation or cardiac function defect during the stages we examined.

FGF16, in particular, is released by cardiomyocytes from the perinatal period and its expression level is increased in the adulthood (Lavine et al., 2005; Hotta et al., 2008; Lu et al., 2008). After FGF16 deletion, the heart also functioned normally but the heart weight and cardiomyocyte number were found to decrease. In addition, the expression level of BNP was significantly downregulated, suggesting that FGF16 might have a specific role in postnatal heart maintenance, especially under pathological conditions (Hotta et al., 2008). Importantly, previous reports showed that FGF2 is expressed in non-cardiomyocytes and has a positive effect on cardiomyocyte replication, angiogenesis, collagen synthesis and infarct repair or hypertrophy (Kaye et al., 1996; Virag et al., 2007; House et al., 2010). It has been reported that FGF16 blocks the FGF2 function by competing with FGF2 for binding to its receptor FGFR1c (FGF receptor-1c) (Lu et al., 2008), which might, therefore, inhibit cardiac hypertrophy and fibrosis (Matsumoto et al., 2013; Santiago et al., 2014). Altogether, previous findings indicate that FGF16 in the extracellular matrix might promote the inhibition of fibrosis and hypertrophy, or provide a niche for cardiac progenitors to drive regeneration. In this study, we revealed that Fgf16 is a direct downstream target of GATA4 and is downregulated in the cardiomyocyte specific Gata4 knockout mouse hearts. In light of the fact that GATA4 is also a regulator of heart hypertrophy (Bisping et al., 2006), we concluded that GATA4 regulate FGF16 expression in cardiomyocytes to control heart hypertrophy after birth. Notably, upregulation of FGF16 partially restored heart function after injury in the absence of GATA4 expression in cardiomyocytes. Overexpression of FGF16 led to downregulation of genes involved in hypertrophy, apoptosis and fibrosis and upregulation of genes associated with cell proliferation in mutant hearts, suggesting that FGF16 is important in preserving heart function. Taken together, our functional analysis demonstrated

that the paracrine factor FGF16 can rescue GATA4-mediated deficiency in cardiomyocytes, at least in part, by promoting cardiomyocyte replication and inhibiting cardiac hypertrophy. Since FGF16 is a secreted protein, identification of its function during neonatal heart regeneration could shed light on development of candidate drugs for protecting the heart from injury.

Acknowledgements

We thank H. Zeng for the Rosa26-RFP mouse line and members of the Zhou laboratory for offering comments in preparation of this manuscript.

Competing interests

The authors declare no competing or financial interests.

Author contributions

W.Y. designed the study, performed experiments and analyzed the data. X.H., X.T., H.Z., L.H., Y.W. bred the mice and performed experiments. Y.N., S.H., Z.L., B.Z., W.P. and K.L. provided valuable comments and reagents, analyzed the data and edited the manuscript. B.Z. conceived and supervised the study, analyzed the data and wrote the manuscript.

Funding

This work was supported by National Science Foundation of China (91339104, 31271552, 31222038, 31301188, 31571503, 31501172), Ministry of Science and Technology (2012CB945102 and 2013CB945302), Shanghai Zhangjiang Stem Cell Research Project (ZJ2014-ZD-002), Shanghai Basic Research Key Project (14JC1407400), China Postdoctoral Science Foundation (2013M541561, 2015M570389, 2015M581669), Youth Innovation Promotion Association of Chinese Academy of Sciences (2015218), Shanghai Yangfan Project (15YF1414000) and Shanghai Rising-Star Program (15QA1404300). Shanghai Institutes for Biological Sciences (SIBS) President Fund, SIBS Postdoc Fund (2013KIP311, 2014KIP314), Sanofi-SIBS Fellowship, Astrazeneca and Research Grants Council of Hong Kong (24110515).

References

Aries, A., Paradis, P., Lefebvre, C., Schwartz, R. J. and Nemer, M. (2004). Essential role of GATA-4 in cell survival and drug-induced cardiotoxicity. *Proceedings of the National Academy of Sciences of the United States of America* **101**, 6975-6980.

Belaguli, N. S., Sepulveda, J. L., Nigam, V., Charron, F., Nemer, M. and Schwartz, R. J. (2000). Cardiac tissue enriched factors serum response factor and GATA-4 are mutual coregulators. *Molecular and cellular biology* **20**, 7550-7558.

Bhalla, S. S., Robitaille, L. and Nemer, M. (2001). Cooperative activation by GATA-4 and YY1 of the cardiac B-type natriuretic peptide promoter. *The Journal of biological chemistry* **276**, 11439-11445.

Bisping, E., Ikeda, S., Kong, S. W., Tarnavski, O., Bodyak, N., McMullen, J. R., Rajagopal, S., Son, J. K., Ma, Q., Springer, Z. et al. (2006). Gata4 is required for maintenance of postnatal cardiac function and protection from pressure overload-induced heart failure. *Proceedings of the National Academy of Sciences of the United States of America* **103**, 14471-14476.

Boheler, K. R., Czyz, J., Tweedie, D., Yang, H. T., Anisimov, S. V. and Wobus, A. M. (2002). Differentiation of pluripotent embryonic stem cells into cardiomyocytes. *Circulation research* **91**, 189-201.

Charron, F., Tsimiklis, G., Arcand, M., Robitaille, L., Liang, Q., Molkentin, J. D., Meloche, S. and Nemer, M. (2001). Tissue-specific GATA factors are transcriptional effectors of the small GTPase RhoA. *Genes & development* **15**, 2702-2719.

Cross, M. J. and Claesson-Welsh, L. (2001). FGF and VEGF function in angiogenesis: signalling pathways, biological responses and therapeutic inhibition. *Trends in pharmacological sciences* **22**, 201-207.

Durocher, D., Charron, F., Warren, R., Schwartz, R. J. and Nemer, M. (1997). The cardiac transcription factors Nkx2-5 and GATA-4 are mutual cofactors. *The EMBO journal* **16**, 5687-5696.

Ford-Perriss, M., Abud, H. and Murphy, M. (2001). Fibroblast growth factors in the developing central nervous system. *Clinical and experimental pharmacology & physiology* **28**, 493-503.

Gonzalez-Rosa, J. M., Martin, V., Peralta, M., Torres, M. and Mercader, N. (2011). Extensive scar formation and regression during heart regeneration after cryoinjury in zebrafish. *Development* **138**, 1663-1674.

Grieger, J. C., Choi, V. W. and Samulski, R. J. (2006). Production and characterization of adeno-associated viral vectors. *Nature protocols* **1**, 1412-1428.

Gupta, V. and Poss, K. D. (2012). Clonally dominant cardiomyocytes direct heart morphogenesis. *Nature* **484**, 479-484.

Gupta, V., Gemberling, M., Karra, R., Rosenfeld, G. E., Evans, T. and Poss, K. D. (2013). An injury-responsive gata4 program shapes the zebrafish cardiac ventricle. *Current biology : CB* **23**, 1221-1227.

Han, C., Nie, Y., Lian, H., Liu, R., He, F., Huang, H. and Hu, S. (2015). Acute inflammation stimulates a regenerative response in the neonatal mouse heart. *Cell research* **25**, 1137-1151.

He, L., Tian, X., Zhang, H., Hu, T., Huang, X., Zhang, L., Wang, Z. and Zhou, B. (2014). BAF200 is required for heart morphogenesis and coronary artery development. *PloS one* **9**, e109493.
Heineke, J., Auger-Messier, M., Xu, J., Oka, T., Sargent, M. A., York, A., Klevitsky, R., Vaikunth, S., Duncan, S. A., Aronow, B. J. et al. (2007). Cardiomyocyte GATA4 functions as a stress-responsive regulator of angiogenesis in the murine heart. *The Journal of clinical investigation* **117**, 3198-3210.
Hotta, Y., Sasaki, S., Konishi, M., Kinoshita, H., Kuwahara, K., Nakao, K. and Itoh, N. (2008). Fgf16 is required for cardiomyocyte proliferation in the mouse embryonic heart. *Developmental dynamics : an official publication of the American Association of Anatomists* **237**, 2947-2954.
House, S. L., House, B. E., Glascock, B., Kimball, T., Nusayr, E., Schultz, J. E. and Doetschman, T. (2010). Fibroblast Growth Factor 2 Mediates Isoproterenol-induced Cardiac Hypertrophy through Activation of the Extracellular Regulated Kinase. *Molecular and cellular pharmacology* **2**, 143-154.
Jesty, S. A., Steffey, M. A., Lee, F. K., Breitbach, M., Hesse, M., Reining, S., Lee, J. C., Doran, R. M., Nikitin, A. Y., Fleischmann, B. K. et al. (2012). c-kit+ precursors support postinfarction myogenesis in the neonatal, but not adult, heart. *Proceedings of the National Academy of Sciences of the United States of America* **109**, 13380-13385.
Kaye, D. M., Kelly, R. A. and Smith, T. W. (1996). Cytokines and cardiac hypertrophy: roles of angiotensin II and basic fibroblast growth factor. *Clinical and experimental pharmacology & physiology* **23 Suppl 3**, S136-141.
Kikuchi, K., Holdway, J. E., Werdich, A. A., Anderson, R. M., Fang, Y., Egnaczyk, G. F., Evans, T., Macrae, C. A., Stainier, D. Y. and Poss, K. D. (2010). Primary contribution to zebrafish heart regeneration by gata4(+) cardiomyocytes. *Nature* **464**, 601-605.
Lavine, K. J., Yu, K., White, A. C., Zhang, X., Smith, C., Partanen, J. and Ornitz, D. M. (2005). Endocardial and epicardial derived FGF signals regulate myocardial proliferation and differentiation in vivo. *Developmental cell* **8**, 85-95.
Liang, Q., De Windt, L. J., Witt, S. A., Kimball, T. R., Markham, B. E. and Molkentin, J. D. (2001). The transcription factors GATA4 and GATA6 regulate cardiomyocyte hypertrophy in vitro and in vivo. *The Journal of biological chemistry* **276**, 30245-30253.
Lin, Z., von Gise, A., Zhou, P., Gu, F., Ma, Q., Jiang, J., Yau, A. L., Buck, J. N., Gouin, K. A., van Gorp, P. R. et al. (2014). Cardiac-specific YAP activation improves cardiac function and survival in an experimental murine MI model. *Circulation research* **115**, 354-363.
Lu, J. R., McKinsey, T. A., Xu, H., Wang, D. Z., Richardson, J. A. and Olson, E. N. (1999). FOG-2, a heart- and brain-enriched cofactor for GATA transcription factors. *Molecular and cellular biology* **19**, 4495-4502.
Lu, S. Y., Sontag, D. P., Detillieux, K. A. and Cattini, P. A. (2008). FGF-16 is released from neonatal cardiac myocytes and alters growth-related signaling: a possible role in postnatal development. *American journal of physiology. Cell physiology* **294**, C1242-1249.
Mahmoud, A. I., Kocabas, F., Muralidhar, S. A., Kimura, W., Koura, A. S., Thet, S., Porrello, E. R. and Sadek, H. A. (2013). Meis1 regulates postnatal cardiomyocyte cell cycle arrest. *Nature* **497**, 249-253.

Matsumoto, E., Sasaki, S., Kinoshita, H., Kito, T., Ohta, H., Konishi, M., Kuwahara, K., Nakao, K. and Itoh, N. (2013). Angiotensin II-induced cardiac hypertrophy and fibrosis are promoted in mice lacking Fgf16. *Genes to cells : devoted to molecular & cellular mechanisms* **18**, 544-553.
Min, H., Danilenko, D. M., Scully, S. A., Bolon, B., Ring, B. D., Tarpley, J. E., DeRose, M. and Simonet, W. S. (1998). Fgf-10 is required for both limb and lung development and exhibits striking functional similarity to Drosophila branchless. *Genes & development* **12**, 3156-3161.
Miyake, A., Konishi, M., Martin, F. H., Hernday, N. A., Ozaki, K., Yamamoto, S., Mikami, T., Arakawa, T. and Itoh, N. (1998). Structure and expression of a novel member, FGF-16, on the fibroblast growth factor family. *Biochemical and biophysical research communications* **243**, 148-152.
Molkentin, J. D., Lin, Q., Duncan, S. A. and Olson, E. N. (1997). Requirement of the transcription factor GATA4 for heart tube formation and ventral morphogenesis. *Genes & development* **11**, 1061-1072.
Monzen, K., Shiojima, I., Hiroi, Y., Kudoh, S., Oka, T., Takimoto, E., Hayashi, D., Hosoda, T., Habara-Ohkubo, A., Nakaoka, T. et al. (1999). Bone morphogenetic proteins induce cardiomyocyte differentiation through the mitogen-activated protein kinase kinase kinase TAK1 and cardiac transcription factors Csx/Nkx-2.5 and GATA-4. *Molecular and cellular biology* **19**, 7096-7105.
Morin, S., Charron, F., Robitaille, L. and Nemer, M. (2000). GATA-dependent recruitment of MEF2 proteins to target promoters. *The EMBO journal* **19**, 2046-2055.
Oka, T., Maillet, M., Watt, A. J., Schwartz, R. J., Aronow, B. J., Duncan, S. A. and Molkentin, J. D. (2006). Cardiac-specific deletion of Gata4 reveals its requirement for hypertrophy, compensation, and myocyte viability. *Circulation research* **98**, 837-845.
Ornitz, D. M. and Itoh, N. (2015). The Fibroblast Growth Factor signaling pathway. *Wiley interdisciplinary reviews. Developmental biology* **4**, 215-266.
Patient, R. K. and McGhee, J. D. (2002). The GATA family (vertebrates and invertebrates). *Current opinion in genetics & development* **12**, 416-422.
Porrello, E. R., Mahmoud, A. I., Simpson, E., Hill, J. A., Richardson, J. A., Olson, E. N. and Sadek, H. A. (2011). Transient regenerative potential of the neonatal mouse heart. *Science* **331**, 1078-1080.
Porrello, E. R., Mahmoud, A. I., Simpson, E., Johnson, B. A., Grinsfelder, D., Canseco, D., Mammen, P. P., Rothermel, B. A., Olson, E. N. and Sadek, H. A. (2013). Regulation of neonatal and adult mammalian heart regeneration by the miR-15 family. *Proceedings of the National Academy of Sciences of the United States of America* **110**, 187-192.
Rojas, A., Kong, S. W., Agarwal, P., Gilliss, B., Pu, W. T. and Black, B. L. (2008). GATA4 is a direct transcriptional activator of cyclin D2 and Cdk4 and is required for cardiomyocyte proliferation in anterior heart field-derived myocardium. *Molecular and cellular biology* **28**, 5420-5431.
Rysa, J., Tenhunen, O., Serpi, R., Soini, Y., Nemer, M., Leskinen, H. and Ruskoaho, H. (2010). GATA-4 is an angiogenic survival factor of the infarcted heart. *Circulation. Heart failure* **3**, 440-450.
Sadek, H. A., Martin, J. F., Takeuchi, J. K., Leor, J., Nie, Y., Giacca, M. and Lee, R. T. (2014). Multi-investigator letter on reproducibility of neonatal heart regeneration following apical resection. *Stem cell reports* **3**, 1.

Santiago, J. J., McNaughton, L. J., Koleini, N., Ma, X., Bestvater, B., Nickel, B. E., Fandrich, R. R., Wigle, J. T., Freed, D. H., Arora, R. C. et al. (2014). High molecular weight fibroblast growth factor-2 in the human heart is a potential target for prevention of cardiac remodeling. *PloS one* **9**, e97281.
Sen, S. and Sadek, H. A. (2015). Neonatal heart regeneration: mounting support and need for technical standards. *Journal of the American Heart Association* **4**, e001727.
Sofronescu, A. G., Detillieux, K. A. and Cattini, P. A. (2010). FGF-16 is a target for adrenergic stimulation through NF-kappaB activation in postnatal cardiac cells and adult mouse heart. *Cardiovascular research* **87**, 102-110.
Sontag, D. P., Wang, J., Kardami, E. and Cattini, P. A. (2013). FGF-2 and FGF-16 protect isolated perfused mouse hearts from acute doxorubicin-induced contractile dysfunction. *Cardiovascular toxicology* **13**, 244-253.
Strungs, E. G., Ongstad, E. L., O'Quinn, M. P., Palatinus, J. A., Jourdan, L. J. and Gourdie, R. G. (2013). Cryoinjury models of the adult and neonatal mouse heart for studies of scarring and regeneration. *Methods in molecular biology* **1037**, 343-353.
Valen, G., Yan, Z. Q. and Hansson, G. K. (2001). Nuclear factor kappa-B and the heart. *Journal of the American College of Cardiology* **38**, 307-314.
Virag, J. A., Rolle, M. L., Reece, J., Hardouin, S., Feigl, E. O. and Murry, C. E. (2007). Fibroblast growth factor-2 regulates myocardial infarct repair: effects on cell proliferation, scar contraction, and ventricular function. *The American journal of pathology* **171**, 1431-1440.
Wang, E., Sun, S., Qiao, B., Duan, W., Huang, G., An, Y., Xu, S., Zheng, Y., Su, Z., Gu, X. et al. (2013). Identification of functional mutations in GATA4 in patients with congenital heart disease. *PloS one* **8**, e62138.
Watt, A. J., Battle, M. A., Li, J. and Duncan, S. A. (2004). GATA4 is essential for formation of the proepicardium and regulates cardiogenesis. *Proceedings of the National Academy of Sciences of the United States of America* **101**, 12573-12578.
Werner, S. and Grose, R. (2003). Regulation of wound healing by growth factors and cytokines. *Physiological reviews* **83**, 835-870.
Wu, B., Zhou, B., Wang, Y., Cheng, H. L., Hang, C. T., Pu, W. T., Chang, C. P. and Zhou, B. (2010). Inducible cardiomyocyte-specific gene disruption directed by the rat Tnnt2 promoter in the mouse. *Genesis* **48**, 63-72.
Yanazume, T., Hasegawa, K., Morimoto, T., Kawamura, T., Wada, H., Matsumori, A., Kawase, Y., Hirai, M. and Kita, T. (2003). Cardiac p300 is involved in myocyte growth with decompensated heart failure. *Molecular and cellular biology* **23**, 3593-3606.
Zeisberg, E. M., Ma, Q., Juraszek, A. L., Moses, K., Schwartz, R. J., Izumo, S. and Pu, W. T. (2005). Morphogenesis of the right ventricle requires myocardial expression of Gata4. *The Journal of clinical investigation* **115**, 1522-1531.

Figures

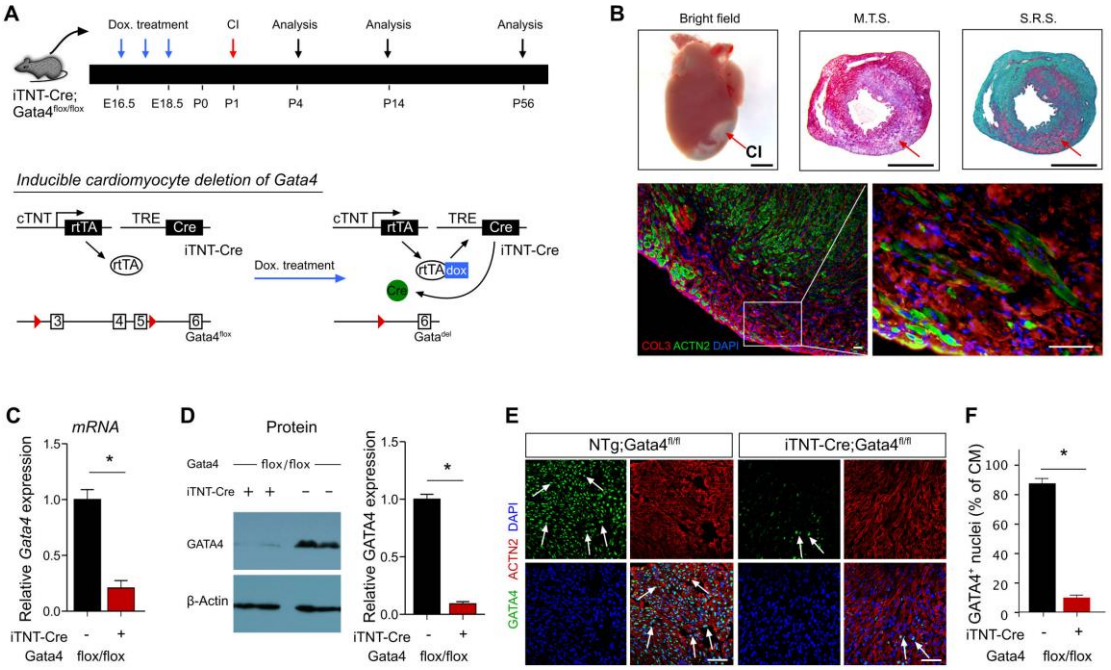

Fig. 1. Perinatal inducible ablation of Gata4 in neonatal cardiomyocytes. (A) Strategy of doxycycline (Dox.) treatement, cryoinfarction (CI) injury model and analysis after CI. iTNT-Cre contains two constructs: the cardi*ac*-specific troponin T promoter driving the reverse tet activator protein rtTA (cTNT-rtTA), and a tet activator protein-dependent promoter driving Cre (TRE-Cre). Dox. treatment leads to Cre expression specifically in cardiomyocytes and results in Cre-mediated removal of floxed exon3-5 of Gata4 gene. **(B)** Whole mount view of P14 heart after CI (red arrow) and sections by Masson Trichrome staining (M.T.S.) and Siruis-red staining (S.R.S). Lower panel shows collagen deposit in CI area. **(C)** Quantitative RT-PCR of *Gata4* mRNA of ventricular extract from iTNT-Cre;Gata4fl/fl neonatal mice or littermate controls non-transgenic (NTg or iTNT-Cre negative) NTg;Gata4fl/fl mice. n = 6. **(D)** Western immunoblotting of GATA4 protein from ventricles. n = 6. **(E)** Immunostaning of GATA4, cardiomyocyte marker ACTN2 and nuclear marker DAPI on neonatal mice heart section. Arrows indicate GATA4+ ACTN2+ cardiomyocytes. **(F)** Quantification of GATA4 positive cardiomyocytes in neonatal heart. n = 6. White bar = 50µm; black bar = 1 mm. * $P < 0.01$; n = 4. Asterisks indicate statistically significant difference compared with controls. Data are mean ± s.e.m.

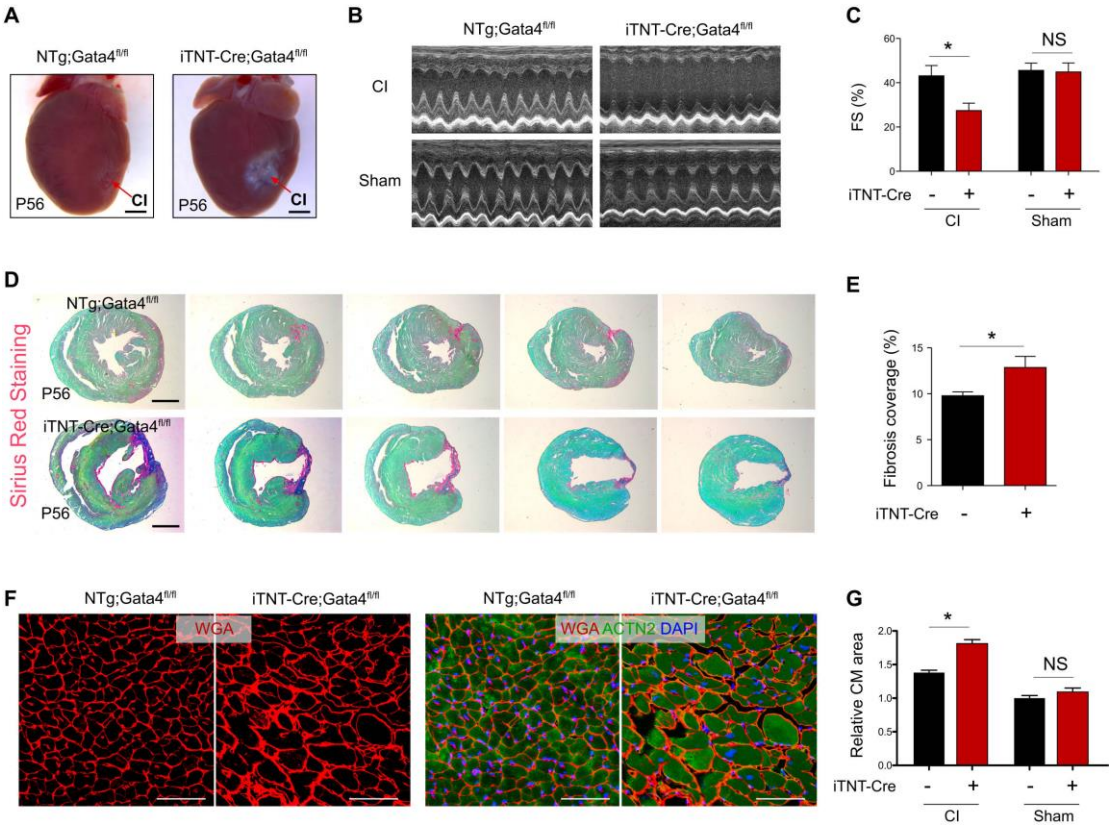

Fig. 2. **Gata4 is required for neonatal heart regeneration after CI. (A)** Whole mount view of P56 heart after CI injury at P1. Red arrows indicate CI injury. **(B,C)** Echocardiographic figure showing severely depressed fractional shortening, a measure of systolic contractile function, in CI- or sham-operated Gata4-KO and control mice. n = 6 - 8. **(D)** Heart cross sections were performed Sirius red staining showing increased fibrosis in the ventricle wall after perinatal removal of Gata4. **(E)** Fibrosis coverage was calculated as fibrotic tissue covered length among the total circumference of heart sections. n = 4 - 6. **(F)** WGA and ACTN2 staining on Gata4 deleted heart sections. **(G)** Quantification of cardiomyocytes (CM) area in CI- or sham-operated Gata4-KO and control mice. n = 4-6. **P* < 0.05; NS, non-significant. Scale bars: 1 mm in A, D; 50 μm in F.

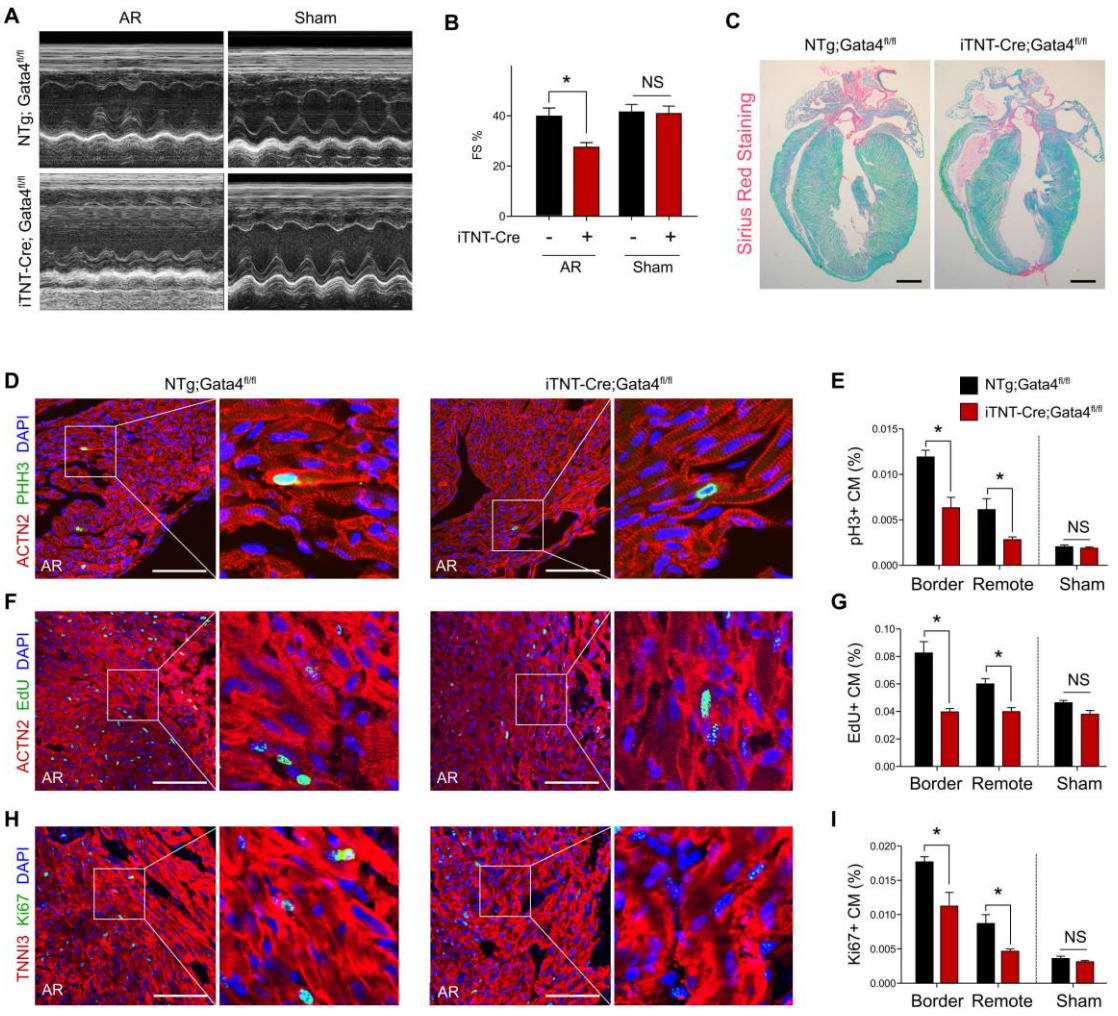

Fig. 3. Gata4 is required for neonatal heart regeneration after apical resection. **(A,B)** Echocardiographic figure showing severely depressed fractional shortening in Gata4 deleted hearts after apical resection (AR). **(C)** Sirius red staining showing increased fibrobsis in the apex after perinatal removal of Gata4. **(D,F,H)** Immunostaining for cell proliferation markers pH3, EdU and Ki67 with cardiomyocyte markers ACTN2 or TNNI3 on heart sections of Gata4 knockout or littermate controls after AR. **(E,G,I)** Quantification of the percentage of proliferating cardiomyocytes in border or remote regions of Gata4 knockout or littermate control hearts after AR or sham. *$P < 0.05$; NS, non-significant; Scale bars: 1 mm in C; 50 µm in D,F,H.

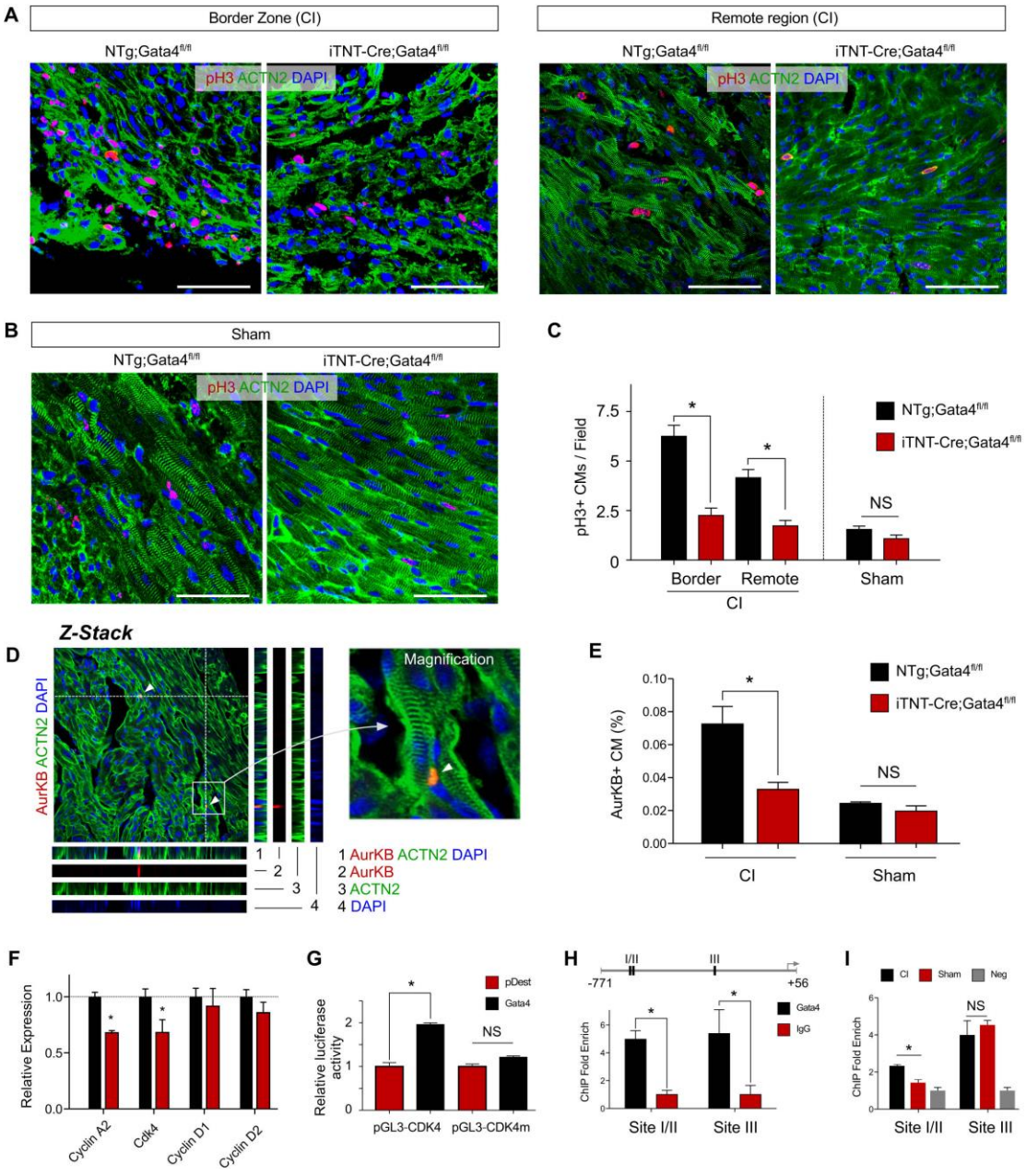

Fig. 4. Reduced cardiomyocytes proliferation in Gata4 ablated CI hearts. (A,B) Immunostaining of phospho-Histone H3 (pH3) and ACTN2 on heart sections containing border zone and remote region after CI or in sham group. **(C)** Quantification of the pH3+ACTN2+ cells in heart sections from CI and Sham groups. n = 4-6. **(D)** Immunostaining of AurKB and ACTN2 on heart sections and cardiomyocyte cytokinesis were detected. White arrow shows cardiomyoctes underwent cytokinesis. **(E)** Quantification of the AurKB+ACTN2+ cells in heart

sections from CI and Sham groups. n = 4 - 6. **(F)** qRT-PCR measurement of cell cycle genes from P9 hearts after CI treatment. **(G)** Luciferase assay showing Gata4 activity on CDK4 promoter. Luciferase activity was normalized to an internal transfection control.*P < 0.05 **(H)** C2C12 cell line were use on ChIP-qPCR to detect Gata4 bound to CDK4 promoters using anti-Gata4 antibody. In addition, nonspecific anti-IgG antibody as negative control. **(I)** ChIP-qPCR analysis on CI- or Sham-operated hearts to detect Gata4 binding enhancement on CDK4 promoter using Gata4 antibody. Gata4-KO hearts (sham) were used as negative controls (Neg). *P < 0.05, NS, non-significant. Data are expressed as mean ± s.e.m. Scale bars, 50 μm.

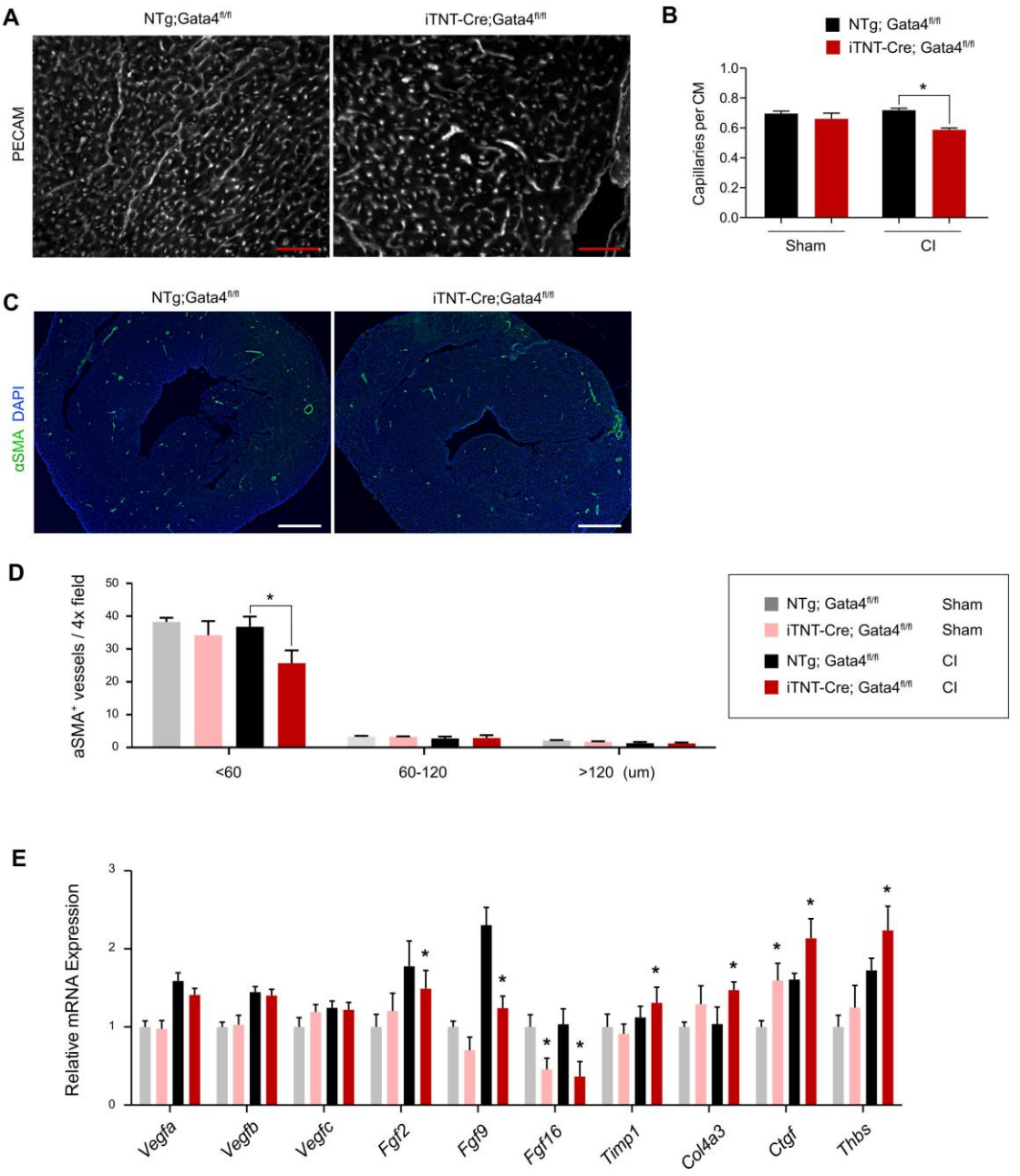

Fig. 5. Coronary angiogenesis and vessel maturation rely on cardiomyocyte specific Gata4 expression during heart regeneration. (A) PECAM staining of injured heart 2 weeks after injury shows reduced capillaries surrounding each cardiomyocyte in the mutant heart compared to the controls. **(B)** Quantitation of capillaries per cardiomyocytes in NTg; Gata4fl/fl or iTNT-Cre; Gata4fl/fl hearts after CI. n = 4 - 6. **(C)** Smooth muscle actin-alpha (αSMA) staining shows reduced small vessels in the Gata4 mutant compared to the Ntg controls. **(D)** Quantitation of vessels

of different size per 4x field in NTg;Gata4fl/fl or iTNT-Cre;Gata4fl/fl hearts. n = 4-6. **(E)** Relative expression of genes encoding angiogenesis-related secreted paracrine factors in NTg;Gata4fl/fl or iTNT-Cre;Gata4fl/fl hearts apex. Gene expression was quantified by qRT-PCR. n = 6 per group. Data are expressed as mean ± s.e.m. * $P < 0.05$. Scale bars: 100 µm in A; 500 µm in C.

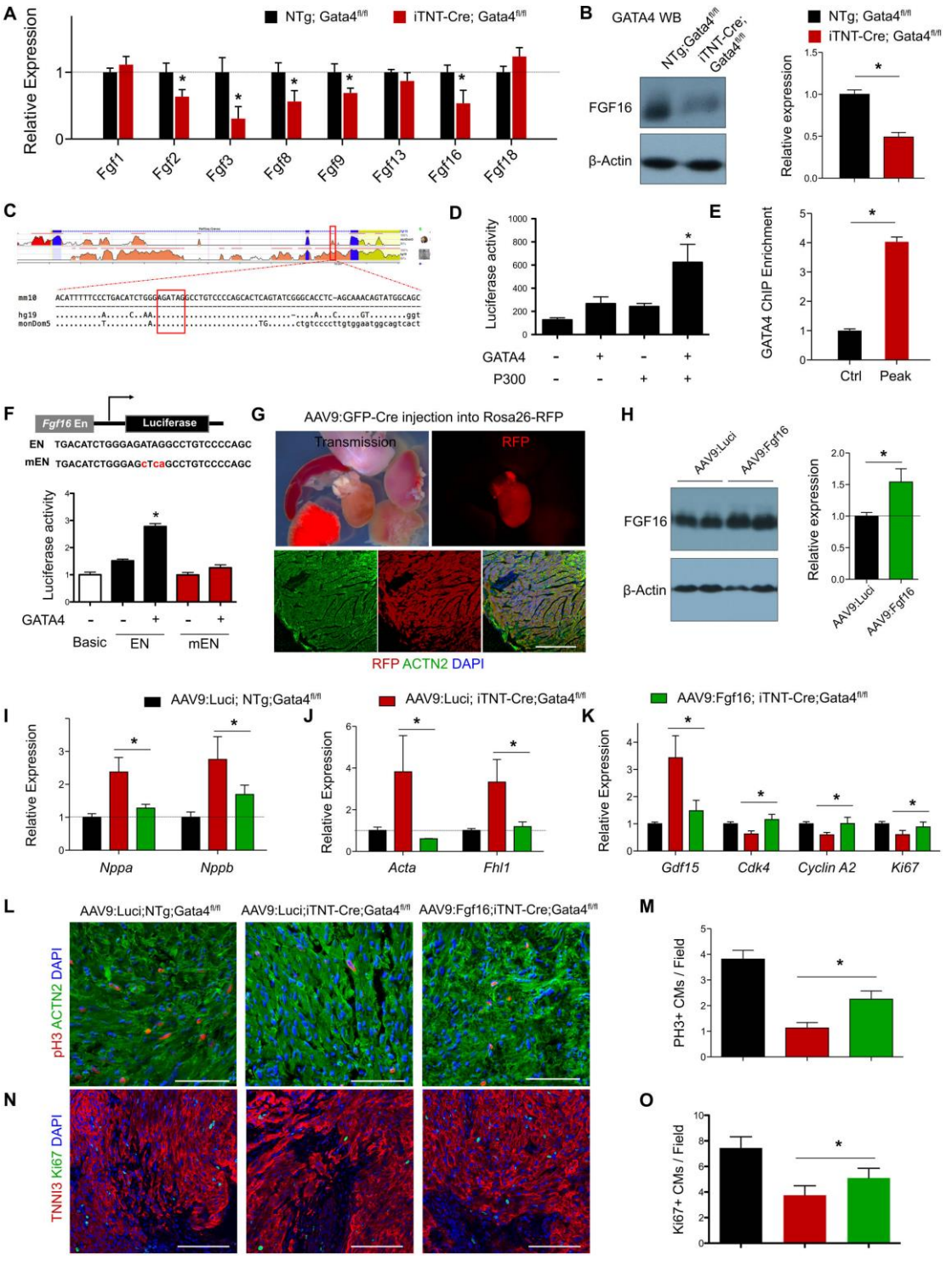

Fig. 6. GATA4 regulates FGF16 expression in vitro and in vivo. (**A**) Relative expression of FGF genes in Gata4 knockout heart apex compared to the controls. Gene expression was quantified by qRT-PCR (n = 6). (**B**) Western immunoblotting of FGF16 protein from 1 week old Gata4 knockout mice and Ntg littermate controls (n =

3). (**C**) ECR browser shows Fgf16 conversation sequence among mouse, opossum and human genomes. Red border-boxes indicate the area containing the conserved GATA binding site. Dots indicate identical sequence between different species. (**D**) A 2000 bp Fgf16 promoter and 1300 bp second intron was cloned into a basic luciferase construct. Neonatal mouse ventricular cardiomyocytes (NMVMs) were transfected with Gata4 or p300 expression constructs and Fgf16 promoter-enhancer luciferase reporter construct as indicated. Luciferase activity was normalized to an internal transfection control. (**E**) Chromatin immunoprecipitation followed by quantitative PCR (ChIP-qPCR) measurement of GATA4 occupancy of the potential conserved peak region and nonspecific control region in neonatal mouse heart. (**F**) A 460 bp region containing the conserved GATA binding site (EN) was cloned into a basic luciferase construct. Mutant version (mEN) contained the base pair mutate as indicated in red. NMVMs were transfected with Gata4 or GFP (as control) expression constructs and wild-type EN or mutant mEN Fgf16 enhancer-luciferase reporter constructs. Luciferase activity was normalized to an internal transfection control. (**G**) Neonatal Rosa-RFP mice were treated with AAV9:GFP-Cre and test at P9. Lung, liver, limb, spleen were used as negative control. Section were stained with ACTN2 show the efficiency of the AAV9 delivery. (**H**) Western blot for FGF16 protein at P9. AAV9:Luci was used as negative control (n = 4). (**I,J**) qRT-PCR measurement of hypertrophic marker gene expression *Nppa*, *Nppb*, *Acta*, *Fhl1* at P9 (n = 6). (**K**) qRT-PCR of proliferation marker genes *Cdk4*, *Cyclin A2*, Ki67 and apoptosis marker gene *Gdf15* in Gata4 knockout heart (n = 6). (**L,N**) Immunostaining for pH3 or Ki67 and ACTN2 on AAV9 treated hearts at P9. (**M,O**) Quantification of proliferating cardiomyocytes percentage. **P* < 0.05, n = 6. Data are mean ± s.e.m. Scale bars, 100 μm in G; 50 μm in L,N.

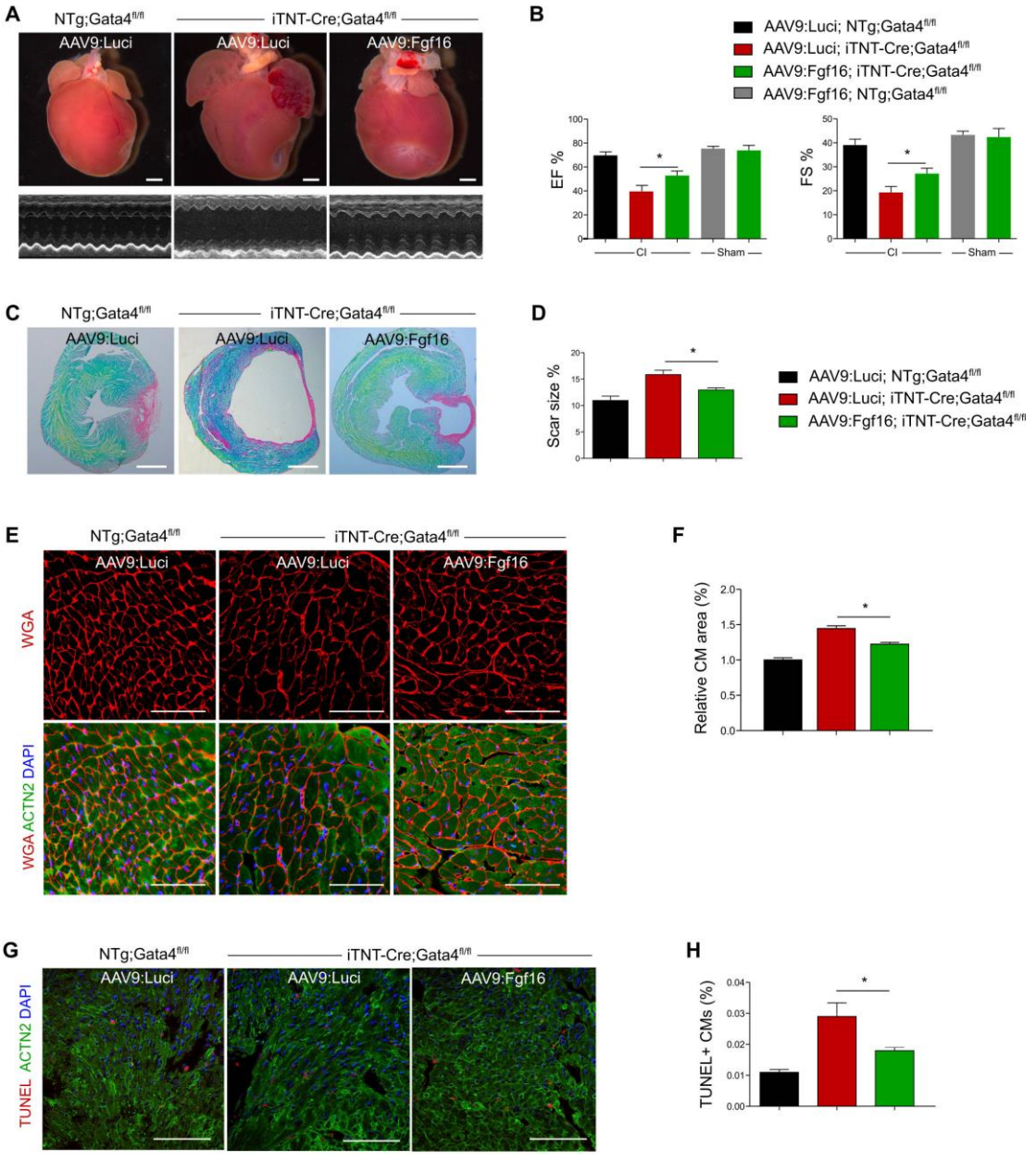

Fig. 7. AAV9:Fgf16 mitigated heart dysfunction in Gata4 knockout mice. (A) AAV9:Fgf16 or AAV9:Luci were administered to Gata4 knockout or control mice at P1 after CI. Echocardiography and heart collection were performed at 8 weeks. **(B)** Echocardiography showing ejection fraction (EF) and fraction shortening (FS). n = 4 - 6 **(C,D)** Sirius red-Fast green staining of heart sections. Scar size was measured as a percentage of ventricular circumference. n = 4 **(E,F)** Immunostaining for WGA and ACTN2 on heart sections to measure CM cross sectioned area. Cross-sectioned area of cardiomyocyte (CM) was measured and compared among three groups. **(G,H)**

Immunostaining of TUNEL and ACTN2 on heart sections (border zone), and quantification of the percentage of apoptotic cardiomyocytes. *$P < 0.05$, n = 4. Data are expressed as mean ± s.e.m. Scale bars: 1 mm in A,C; 50 µm in E,G.

Table S1. Echocardiographic parameters

	CI		Sham	
	Cre+	**Cre-**	**Cre+**	**Cre-**
n	8	6	6	6
HR (BMP)	408.12± 37.9	453.16± 45.96	459± 18.9	418.66± 24.62
LVAW;d (Depth, mm)	0.59± 0.04	0.69± 0.04	0.7± 0.02	0.72± 0.01
LVID;d (Depth, mm)	4.17± 0.11[A]	3.68± 0.18	3.36± 0.12	3.73± 0.02
LVPW;d (Depth, mm)	0.6± 0.03[A]	0.75± 0.05	0.63± 0.03	0.67± 0.03
LVAW;s (Depth, mm)	0.95± 0.09	1.17± 0.1	1.16± 0.06	1.19± 0.06
LVID;s (Depth, mm)	3.04± 0.2[A]	2.11± 0.25	1.85± 0.16	2.03± 0.13
LVPW;s (Depth, mm)	0.89± 0.07[A]	1.18± 0.11	1.03± 0.07	1.12± 0.07
LV Vol;d (ul)	77.96± 5.03[A]	58.83± 6.89	46.58± 4.25[A]	59.36± 0.79
LV Vol;s (ul)	38.12± 5.77[A]	19.08± 6.21	11.35± 2.7	13.76± 2.17
%EF	52.6± 5.23[A]	73.57± 5.5	76.17± 4.75	76.98± 3.43
% FS	27.42± 3.35[A]	43.13± 4.66	44.88± 4.02	45.6± 3.27
LV Mass (AW) (mg)	87.68± 5.81	89.66± 6.03	69.53± 6.1	86.85± 2.63
LV Mass (AW) Corrected (mg)	70.14± 4.65	71.72± 4.82	55.62± 4.88[A]	69.48± 2.1

[A]$P < 0.05$ versus Cre+, Luc line. Cre+, iTnt-Cre;Gata4fl/fl; Cre-, NTg;Gata4fl/fl.

Table S2. Primer sequences used in qRT-PCR

Gene	Forward	Reverse
Gata4	AAACGGAAGCCCAAGAACCTGAAT	GAGCTGGCCTGCGATGTCTGAGTG
Cyclin A2	GGCTGACACTCTTTCCG	CTGGTAGCAAGAATTAGAGCAT
Cyclin D1	TGAGAACAAGCAGACCATCC	TGAACTTCACATCTGTGGCA
Cyclin D2	CACCGACAACTCTGTGAAGC	CCACTTCAGCTTACCCAACA
Cdk4	GGGACATCAAGGTCACCCTA	CGCTTAGAAACTGACGCATT
Gdf15	GAGGACTCGAACTCAGAACCAAGT	CCGGTTGACGCGGAGTAG
Anf	GTGTACAGTGCGGTGTCCAA	ACCTCATCTTCTACCGGCATC
Bnp	ACAAGATAGACCGGATCGGA	AGCCAGGAGGTCTTCCTACA
Acta	AGGCGGTGCTGTCTCTCTAT	GACATTGTGGGTGACACCAT
Fhl1	ACTGCGTGGATTGCTACAAG	TTTACCAAACCCAGTGATGG
Thbs1	CCCTGATGGTAGCTGGAAAT	CTCATCGACGTCTTTGCACT
Timp1	ATATCCGGTACGCCTACACC	GCCCGTGATGAGAAACTCTT
Col4a3	TTAAGTTCAGGCTGGTGCTG	GCATGTCTCAGCTCAGGTGT
Fgf1	AGCTTTCTCCCAAGAGACCA	TCATGGCGTTTGTGTCCTAT
Fgf2	CAACCGGTACCTTGCTATGA	TCCGTGACCGGTAAGTATTG
Fgf3	ACCTGGTGCCCAGAGACCTT	GCAGGAAGAGAGAGGACTTTTGTG
Fgf8	GCTCATTGTGGAGACCGATACTT	TGGCAATTAGCTTCCCCTTCT
Fgf9	GCGGTGGGTTCTTATTGATT	AAATTGGCAAGTCCTCATCC
Fgf12	ATTCCTCAACCCTGTATCGC	ATGAGATGAGGGCTTGGTTT
Fgf13	TATCACCCATATTAAAGCCCCATAA	AAAATTTGGCAGTCCTTCTTCCA
Fgf16	CCATGACTCAAGGGAGCTTT	CTATGCCCAATCCTGAAGGT
Fgf18	AGGAAGAATCTCTATTTTTGTACATTGTGT	GTTCAGGTCAACAGTGGAATCCTA
Vegfa	GAGGATGTCCTCACTCGGAT	TCTCAGACCACACTGAAGCC
Vegfb	AGCCACCAGAAGAAAGTGGT	GCTGGGCACTAGTTGTTTGA
Vegfc	CCCAAACCAGTCACAATCAG	GGTAATGTTGCTGGCAGAGA
Gapdh	GAAGGGCTCATGACCACAG	GATGCAGGGATGATGTTCTG

Primer sequences used in ChIP-qPCR

GATA Site on	Forward	Reverse
***Fgf16* Enhancer**	CCCGGTCAACTATGAGAAGG	GCCTGTCAGTTGGAAAGCTC
Fgf16 Control	TTTTCGCTTCCTCAGACCCCTGTG	TTCTCTGGCCCAAAAGAGGCTG

Primer sequences used in amplifying fragment

Fragment	Forward	Reverse
***Fgf16* Promoter**	CTAGCTAGCTATGCTCATTGGTGTTCCGC	CCCAAGCTTGTCGGCGGCGCTCGCTTGCTC
***Fgf16* Intron**	CTAGCTAGCGTAAGTTCCAACCTTTCTAT	CCCAAGCTTGTTTCTTCTGTGAGGGTGAG
***Fgf16* Enhancer**	CTAGCTAGCGAATGAGGGTTCCAGGGAC	CCCAAGCTTCTATATAAAGCTGCATGGG